Stronger Interlayer Interactions Contribute to Faster Hot Carrier Cooling of Bilayer Graphene under Pressure

Kun Ni,[1,*] Jinxiang Du,[1,*] Jin Yang,[2,*] Shujuan Xu,[2] Xin Cong,[3] Na Shu,[1] Kai Zhang,[2] Aolei Wang,[4] Fei Wang,[1] Liangbing Ge,[1] Jin Zhao,[4,5] Yan Qu,[6] Kostya S. Novoselov,[7] Pingheng Tan,[3] Fuhai Su,[2,†] and Yanwu Zhu[1,‡]

[1]*Hefei National Research Center for Physical Sciences at the Microscale, and CAS Key Laboratory of Materials for Energy Conversion, and Department of Materials Science and Engineering, and iChEM, University of Science and Technology of China, Hefei, Anhui 230026, People's Republic of China*

[2]*Key Laboratory of Materials Physics, Institute of Solid State Physics, HFIPS, Chinese Academy of Sciences, Hefei 230031, China*

[3]*State Key Laboratory of Superlattices and Microstructures, Institute of Semiconductors, Chinese Academy of Sciences, Beijing 100083, People's Republic of China*

[4]*Department of Physics, CAS Key Laboratory of Strongly-Coupled Quantum Matter Physics, and ICQD/Hefei National Laboratory for Physical Sciences at Microscale, University of Science and Technology of China, Hefei, Anhui 230026, China*

[5]*Department of Physics and Astronomy, University of Pittsburgh, Pittsburgh, Pennsylvania 15260, USA and Synergetic Innovation Center of Quantum Information and Quantum Physics, University of Science and Technology of China, Hefei, Anhui 230026, China*

[6]*The Sixth Element (Changzhou) Materials Technology Co., Ltd., Changzhou 213100, China*

[7]*National Graphene Institute, University of Manchester, Oxford Road, Manchester M13 9PL, United Kingdom, Centre for Advanced 2D Materials, National University of Singapore, 117546 Singapore and Chongqing 2D Materials Institute, Liangjiang New Area, Chongqing 400714, China*

(Received 6 July 2020; revised 4 November 2020; accepted 11 December 2020; published 13 January 2021)

We perform femtosecond pump-probe spectroscopy to *in situ* investigate the ultrafast photocarrier dynamics in bilayer graphene and observe an acceleration of energy relaxation under pressure. In combination with *in situ* Raman spectroscopy and *ab initio* molecular dynamics simulations, we reveal that interlayer shear and breathing modes have significant contributions to the faster hot-carrier relaxations by coupling with the in-plane vibration modes under pressure. Our work suggests that further understanding the effect of interlayer interaction on the behaviors of electrons and phonons would be critical to tailor the photocarrier dynamic properties of bilayer graphene.

DOI: 10.1103/PhysRevLett.126.027402

Introduction.—Graphene, with its high electronic mobility (routinely exceeding 10 000 $cm^2 V^{-1} s^{-1}$) and a constant adsorption (~2.3%) for light from ultraviolet to infrared, has been considered for a number of electronic and optoelectronic applications, especially for those where high speed is required [1]. Optoelectronic properties of graphene at short timescales are determined by the dynamics of hot carriers, which is pivotal for such processes as the energy transfer [2], high-harmonic wave generation [3,4], high-field electron transport [5], as well as photothermoelectric effect [6]. Understanding of the dynamics of energy relaxation of hot carriers is crucially important for the design of graphene based photoelectronic devices which utilize such properties as light harvesting, energy upconversion, and thermoelectric photodetection. The hot-carrier dynamics in single layer graphene (SLG) and multilayer graphene (MLG) have been extensively investigated by means of diverse ultrafast optical methods such as transient absorption, time-resolved terahertz spectroscopy, time- and angle-resolved photoemission spectroscopy, etc. [7–14]. It has been established that the photocarrier dynamics in graphene are mainly governed by a rapid thermalization through electron-electron (*e*-*e*) scattering and optical phonon emission on the subpicosecond scale, and a subsequent slower electron-phonon (*e*-ph) scattering through low-frequency acoustic phonons [7,8,15–18], or disorder-assistant acoustic phonons [19,20].

Attempts to investigate the influence of the hopping parameters on the hot-carrier dynamics have been undertaken both for bilayer graphene (BLG) and MLG [13,14,17,21]. The case of BLG is especially interesting as it allows controllable gap opening with transverse electric field and fine control over the *e*-*e* correlation phenomena [22–25]. Thus, Ulstrup *et al.* [13] observed an increased carrier lifetime in BLG compared with zero-gap MLG due to the opening of a small band gap at the Dirac point. Mihnev *et al.* [14] investigated the interlayer thermal transport in epitaxial MLG along the stacking direction by time resolved terahertz and optical pump-probe spectroscopy. Such cross-plane energy transfer, only occurring at low temperatures, stems from the difference in the phonon relaxation rate between layers associated with gradient carrier density distribution. These works emphasized the roles of Coulomb interactions between adjacent

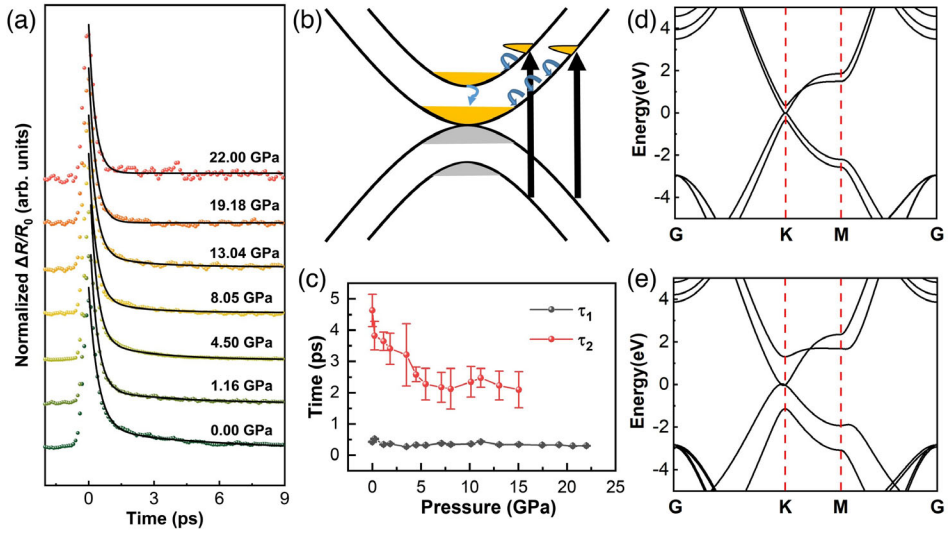

FIG. 1. OPPS results and calculated electronic energy bands of BLG. (a) Transient differential reflectivity of BLG excited by 800-nm pump pulse under pressure. (b) Schematic of excitation and relaxation of electrons in BLG. (c) Fast and slow relaxation time constants fitted by the biexponential function. τ_1 indicates the time for the fast relaxation and τ_2 the time for the slow relaxation. Calculated electronic energy bands of BLG under pressure of (d) 0 GPa and (e) 33.6 GPa.

layers in the photocarrier dynamics of graphene. Still the detailed study of the influence of the interlayer hopping parameters [determined by the local van der Waals (vdW) interaction] on the electron dynamics in graphene structures is missing, mostly due to the difficulties of controlling such parameters.

Herein, we utilize a high-pressure diamond anvil cell (DAC) to control interlayer hopping parameters and study their influence on the ultrafast carrier dynamics of BLG. The hydrostatic pressure created by DAC provides a clean route to modify the vdW interaction in two-dimensional (2D) materials [26,27]. Experimentally, we use near-infrared optical pump-probe spectroscopy (OPPS) in DAC to access the photocarrier dynamics of BLG under high pressures. We find that the energy relaxation through acoustic phonon scattering is reduced dramatically with increasing pressure. High-pressure Raman spectroscopy and density functional theory (DFT) calculations demonstrate that such hydrostatic pressure leads to the increase in the vdW interaction, and therefore elevates the phonon energies of breathing and shear modes, providing possible intermediate phonon scattering path between high-frequency optical phonon and acoustic phonon. Furthermore, *ab initio* molecular dynamics (AIMD) simulations show that the breathing and shear modes contribute much more to the interband relaxation of hot electrons with the assistance of in-plane optical phonon vibrations with increasing pressure. Our work reveals a new carrier cooling channel through the stronger interlayer vdW interaction under pressure, therefore provides valuable insights for the development of graphene-based photoelectric and thermalelectric devices.

Results and discussion.—To investigate the ultrafast photocarrier dynamics of compressed graphene, we carried out OPPS in reflection geometry under pressure generated in DAC, as schematically shown in Fig. S1. More experimental details are provided in the Supplemental Material [28]. A graphene flake, consisting of SLG and BLG regions, was transferred onto one diamond culet of DAC, as shown in Fig. S2 [29]. Raman spectra and corresponding mapping of relative intensity in Fig. S3 shows the good quality of the sample.

Figure 1(a) displays the differential reflectivity (DR) transients, i.e., $|\Delta R/R_0| = |(R - R_0)/R_0|$, as a function of pump-probe delay under different pressures, where R or R_0 is the reflectivity with or without pump, respectively. With increasing pressure, the DR signal declines dramatically, likely due to the increased scattering of silicon oil and diamond [30]. For comparison, each DR curve is normalized by its peak value. As can be seen, the DR signal rises rapidly after photoexcitation followed by a slower decay, corresponding to the hot-carrier formation and subsequent cooling.

Figure 1(b) schematically describes the excitation and relaxation of electrons in BLG for the 800-nm laser pump. Different from SLG, the interlayer coupling of BLG results in the double branches and parabolic relation near the K point both in conduction and valence bands. Upon the irradiation, electrons in two branches of the valence band of BLG absorb the photon energy (~1.55 eV) and instantly get excited to the unoccupied states in the corresponding conduction bands [13]. The subsequent formation of the quasi–Fermi Dirac (QFD) distribution of hot electrons and holes with separated chemical potentials occurs within 10–50 fs via electron-electron (e-e) scattering [8,31], which cannot be resolved in our current experiment using a pulse of 150 fs. Thereby, the initial maximum of DR corresponds

to the establishment of merged hot plasma with the consensus electron temperature and chemical potentials between electrons and holes. It is well known that the energy relaxations of hot carriers through intraband and interband transition in graphene are mainly mediated by the electron-optical phonon (e-optical ph) and electron-acoustic phonon (e-acoustic ph) coupling [7,8,15–18].

As shown in Fig. 1(a), the decay curve is composed of two components, which can be well described by a biexponential function. The obtained fast (τ_1) and slow (τ_2) time constants have the timescale of subpicosecond and a few picoseconds, corresponding to the e-optical ph and e-acoustic ph scattering process, respectively. These time constants approach the earlier reported values in Ref. [7]. In Fig. 1(c), τ_1 and τ_2 are plotted as the function of pressure. With an increase in the pressure, τ_1 maintains a nearly constant value, while the τ_2 value shows an obvious decrease. The drop of τ_2 is especially visible for the pressure between 0 and ~10 GPa. For the pressure above 15 GPa, the two decay components start to merge into one and the DR signal can be reproduced by a single exponential function. We have repeated the OPPS measurements under high pressures up to 14 GPa for SLG (Fig. S4). In contrast to the situation for BLG, both τ_1 and τ_2 do not show obvious pressure dependence. It is worth noting that the obtained τ_2 of SLG is somewhat shorter than that of BLG under low pressures. This may be caused by stronger acoustic phonon scatterings since the BLG show multiple subband structure as elucidated in Fig. 1(b).

To understand such pressure-induced faster relaxation of hot carriers in BLG, several factors are considered: (i) enhancement of e-e Coulomb interactions; (ii) defect scattering; (iii) changes in the electronic structure with pressure; (iv) changing of the phonon spectra. To elucidate on the first two factors, we examine the pump power dependence of photocarrier dynamics under 12.35 GPa. As the incident pump power is increased from 2.5 to 6.5 mW, the peak value of the DR curve demonstrates a linear increase and the relaxation lifetime remains almost unchanged (Fig. S5), indicating that the photocarrier density does not reach saturation in the pump scale studied. Considering that the increasing attenuation of laser power with pressure, neither e-e scattering nor Auger recombination contributes to the additional carrier relaxation under high pressures. In addition, if the energy relaxation through carrier-defect scattering dominates, the lifetime should generally become longer with increasing pump level due to the filling effects of the available defect states [32]. Therefore, the weak pump fluence dependence of time constant can exclude the carrier-defect scattering effects.

To understand the influence of the changes of the band structure on the relaxation time we performed the DFT simulations of the electronic band structure of BLG under pressure (see Supplemental Material [28] for the simulation model and detailed methods [33–39]). Figures 1(d) and 1(e) show the calculation results under 0 GPa and those of 33.6 GPa, respectively. As shown in Fig. 1(d), the BLG at 0 GPa possesses a band structure with a parabolic dispersion, composed of a double-decked subband structure of valance band and conduction band [40]. On the other hand, the high pressure leads to the augment of separation of subbands, i.e., the second conduction band moving upward while the second valance band moves downward, as presented in Fig. 1(e). Thus, it is anticipated that the photocarrier lifetime should initially show an increase with increasing pressure because of the reduction of the width of the subband, which reduces the role of the optical phonons and requires more acoustic phonons to assist the energy relaxation. Therefore, our observed pressure behavior of photocarrier dynamics in BLG cannot be fully explained in terms of energy band changes.

Thus, we focus our attention on the changes in the phonon spectrum and its influence on the electron relaxation time. In general, as for the energy relaxation through optical phonon coupling, the electrons capable of emitting optical phonons should lie in the high-energy tail of the QFD distribution and have the energy higher than participated phonon with energy of $\hbar\omega_O$ [19]. The high-frequency optical phonon (TO and LO) with $\hbar\omega_O \sim 200$ meV would dominate the energy relaxation process. As the electron energy is reduced below $\hbar\omega_O$, the energy relaxation through $\hbar\omega_O$ will be less efficient and the electron cooling channel is restricted to the slow low-frequency acoustic phonon coupling. On the other hand, our DFT calculations do not show obvious changes in acoustic phonon dispersion in the studied pressure range (Fig. S6). Therefore, the acoustic phonon scattering cannot fully explain the acceleration of photocarrier relaxation. For BLG under pressure, we suggest that the shear and breathing modes, governed by vdW interaction, participate in the photocarrier relaxation.

Thereby, we proceed to investigate the pressure dependence of the shear and breathing modes, and their contribution to the hot-carrier cooling. To reveal the modes under pressure, we perform the *in situ* high-pressure Raman spectroscopy and DFT calculations for phonon structures. Figure 2(a) shows the evolution of low frequency mode with pressure. For pressures lower than 8 GPa, it is difficult to distinguish any Raman modes from noise in the range of interest. Under 8.6 GPa a mode at ~67 cm^{-1} appears, which shifts to ~94 cm^{-1} for 21.4 GPa. The enhancement in Raman intensity of shear mode under pressure has also been observed in graphite [41] and boron nitride [42], assigned to pressure-induced transition resonance and enhanced mode polarizability, respectively. We speculate that the similar resonance effect also occurs in BLG under high pressures in view of the pressure-induced separation of subbands as revealed by the calculated band structures. Other pressure-induced effects such as the increased Raman cross-section from the stronger interlayer coupling and the enhanced electron-phonon coupling could also

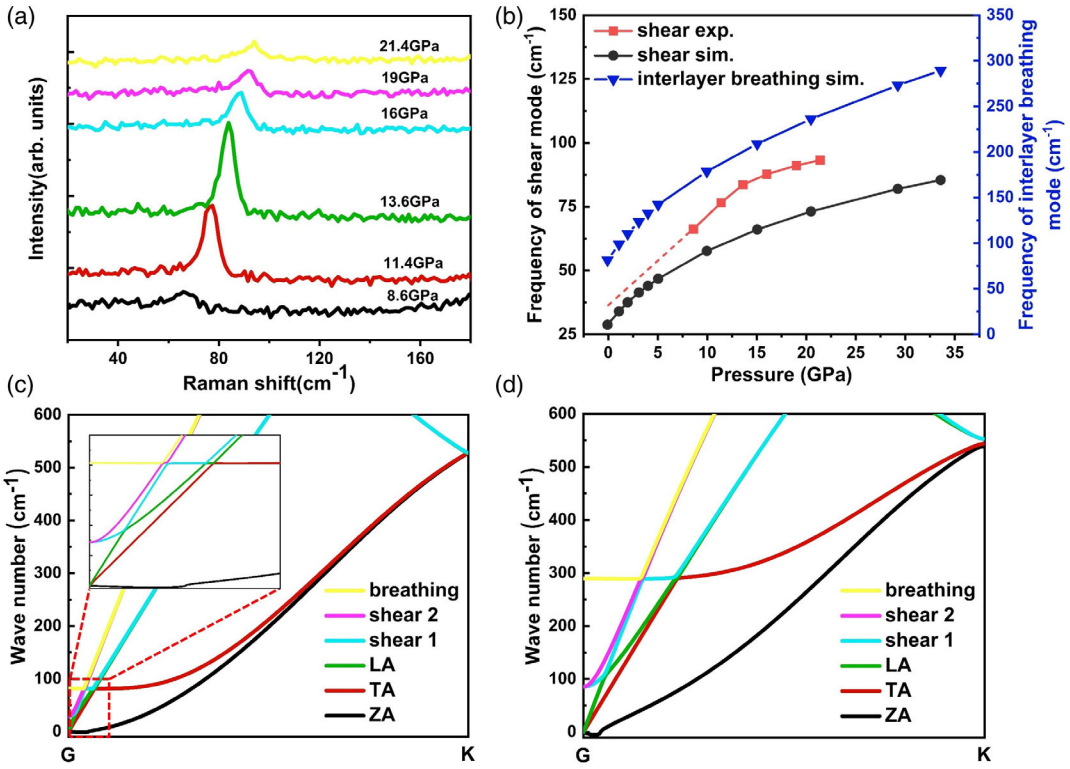

FIG. 2. *In situ* Raman and calculated phonon dispersion of BLG. (a) Raman spectra of BLG with highlighting the shear mode under high pressures. (b) Frequencies of the shear mode obtained from experiment and simulation, as well as the frequency of interlayer breathing mode from simulation as a function of pressure. Calculated phonon dispersion curves of low-frequency modes in BLG under pressure of (c) 0 GPa and (d) 33.6 GPa. The inset in (c) magnifies the dispersion curves nearby the G point.

contribute to the pressure dependence of Raman intensity. The frequency of the Raman mode is extrapolated to $\sim$29 cm^{-1} in DFT simulation (based on the phonon spectrum) or $\sim$36 cm^{-1} in the experiment under 0 GPa, respectively, as shown in Fig. 2(b), indicating that experimentally observed mode in Fig. 2(a) is likely assigned as the interlayer shear mode, close to the reported value of $\sim$31 cm^{-1} [40,43,44]. Figure 2(b) also shows that both the interlayer breathing mode and shear mode shift to higher frequencies under high pressures, which is induced by the enhancement of vdW interaction. It should be noticed that the interlayer breathing mode was not observed in our Raman experiment. The DFT calculation also provides the phonon dispersions under pressure as illuminated in Fig. S6 for full Brillouin zone range, and Figs. 2(c) and 2(d) ranging from G (zone center) to K point to show the details of low-frequency modes. By comparing the phonon dispersions of BLG with and without pressure, one can see that the breathing mode lifts quickly from $\sim$81 to $\sim$273 cm^{-1} and the shear mode from 29 to 82 cm^{-1}.

Earlier theory shows that the cooling power, associated with the photocarrier relaxation rate, should increase with increasing optical phonon frequency in graphene [45]. Compared with low-frequency phonon, the optical phonon with higher frequency would cost more energy of electrons by phonon emission in each scattering event, and produces faster energy exchange rate between lattice and electron. From our high-pressure Raman spectra and DFT calculation, the frequency of both shear and breathing modes increases with pressure. Consequently, the carrier cooling process becomes faster since these phonon modes provide more intraband scattering channels, and shall act as intermediates to bridge the high-frequency e-optical ph and low-frequency e-acoustic ph scattering toward more efficient energy relaxation. This is consistent with the decrease of relaxation time constant with increasing pressure.

On the other hand, the energy relaxation through interband transition should also take nontrivial role in hot carrier cooling of BLG due to its multiple subband structure. For instance, as the frequency of breathing mode moves toward lattice energy of $k_B T_L$ ($T = 300$ K) with increasing pressure, more phonons are activated. Consequently, the lattice vibration with higher frequency and larger amplitude allows for the elevation of nucleus velocity and modulation of coupling between electric states [46], and may facilitate the hot carrier cooling. To evaluate such interband relaxation dynamic assisted by interlayer vibration, we carry out *ab initio* molecular dynamics (AIMD) calculations (see Fig. 3 and Supplemental Material at [28] for the AIMD simulation methods and the detailed models and the selected bands in Fig. S7). From the time-dependent electron energy states of BLG in Figs. 3(a) and 3(c), we

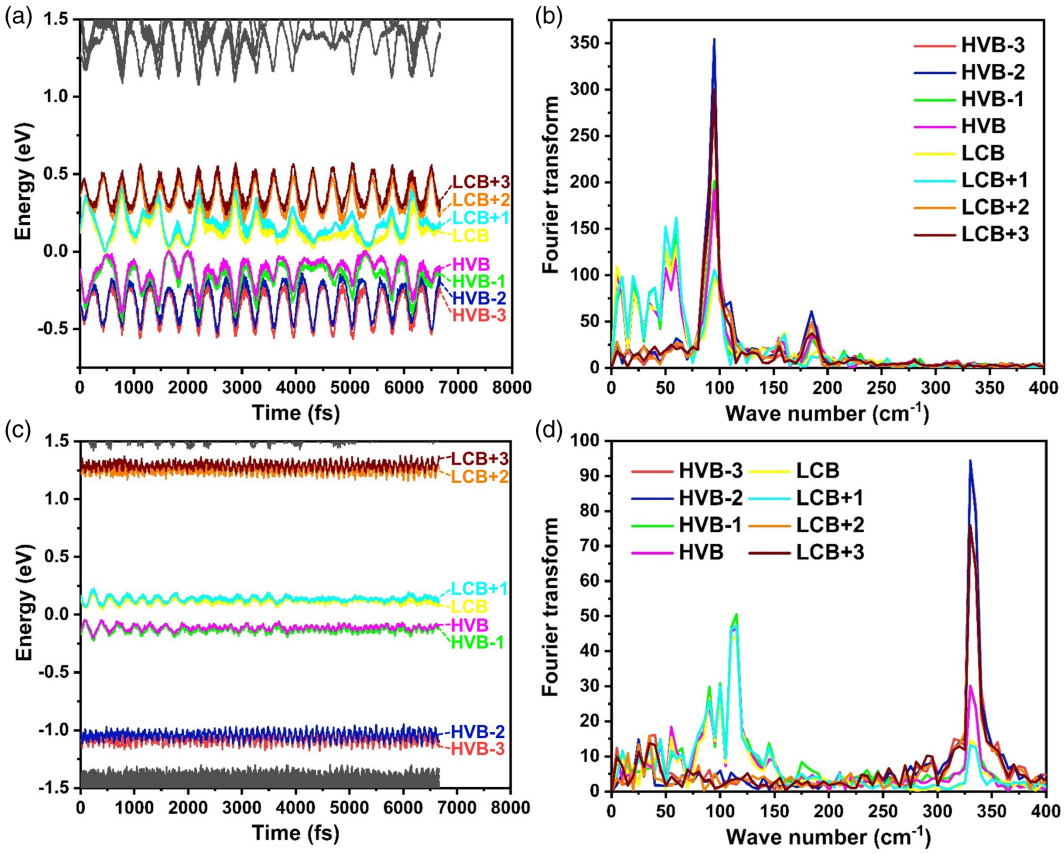

FIG. 3. Time-dependent electron energy levels and the corresponding FFT spectra of BLG under pressure. (a) Time evolution of electron energy bands of BLG under 0 GPa and (b) FFT spectra from three bands below highest valance band (HVB) to three bands above lowest conduction band (LCB). (c) Time evolution of electron energy states of BLG under a pressure of ~32 GPa and (d) FFT spectra from three bands below HVB to 3 bands above LCB.

can see that the electron energy shows periodic vibrations due to the phonons described by MD simulation, leading to the dynamic *e*-ph coupling [47,48]. To identify the most prominent vibration frequency, fast Fourier transformation (FFT) was performed and the results are shown in Figs. 3(b) and 3(d). For BLG at 0 GPa, the coupling is mainly attributed to the phonons with frequency of ~95 and ~55 cm^{-1}. The frequency of ~95 cm^{-1} is highly consistent with the frequency of ~95.1 cm^{-1} of the interlayer breathing mode obtained by calculating the averaged interlayer spacing in MD simulation, as shown in Figs. S8(a) and S8 (b). The frequency of ~55 cm^{-1} shall be attributed to the interlayer shear mode with frequency of 29 cm^{-1} in the static phonon dispersion shown in Fig. 2(c), considering the calculation errors for low-energy phonons. For BLG under ~32 GPa, the main coupling peaks move to the higher frequencies at ~330 and ~101 cm^{-1}. The frequency of ~330 cm^{-1} fits well with the interlayer breathing frequency of 330.3 cm^{-1}, as shown in Figs. S8(c) and S8(d), and the frequency of ~101 cm^{-1} is close to the interlayer shear mode at 85 cm^{-1} in the static phonon dispersion in Fig. 2(d). In addition, a calculation of energy evolution in the relaxation with frozen phonon method under 0 GPa also shows that, both the LB and shear modes provide a quick relaxation channel only when being coupled with the in-plane optical modes [Figs. S9(a) and S9(b)]. If the in-plane optical modes are not involved, the bare interlayer breathing mode can hardly provide relaxation while the bare shear modes provide a slow relaxation [Figs. S9(c) and S9(d)]. The higher vibration frequencies of interlayer modes indicate the higher nuclear velocity due to the stronger interlayer coupling under pressure, in contrast to the in-plane phonons whose frequency does not increase substantially with pressure (Fig. S10). A previous study shows that the electron transition probability positively correlates to the nuclear motion velocity in the ultrafast relaxation [39]. Combining nonadiabatic molecular dynamics simulations and frozen phonon models, we found that the increasing frequency of LB model could help to make the relaxation faster, as shown in Fig. S11. Thus, the faster interband relaxation under pressure is mainly attributed to the higher frequency of the interlayer coupling phonons, including shear and breathing phonons, but the coupling between in-plane and out-of-plane modes is necessary.

Conclusion.—In conclusion, we have carried out experimental and theoretical investigations on the ultrafast relaxation dynamics of nonequilibrium photocarriers in BLG under high pressures. The pressure dependence of photocarrier dynamics accessed by OPPS is featured with significant drop in carrier lifetime in BLG. High-pressure Raman spectroscopy and DFT calculations demonstrate that high pressure increases the energies of low-frequency interlayer modes, including interlayer breathing and shear modes. By combining AIMD, which allows for the simulation of electronic states in time domain under high pressures, we establish that the low-frequency interlayer phonon modes, governed by the vdW interaction, play an indispensable role in the energy relaxation of hot carriers in BLG. Our work unravels a new carrier cooling pathway through the interlayer vdW interaction, which bridges the relaxation channel between high-energy optical and low-energy acoustic phonon scatterings. We believe the result would make a step toward understanding the electron-phonon coupling behavior in BLG, thus shedding light on future research in related topics, such as light-harvesting, thermoelectric detection, and terahertz emission devices.

This work was supported by National Key R&D Program of China (Grant No. 2020YFA0711502), Natural Science Foundation of China (No. 51772282, No. 51972299, No. 11774354, No. 51727806, No. 52003265), and funding from Hefei Center for Physical Science and Technology. The authors thank the Ruoff Group (IBS CMCM Center; supported by IBS-R0190D1) located at UNIST, for providing the BLG samples.

*These authors contributed equally to this work.
†To whom all correspondence should be addressed. fhsu@issp.ac.cn
‡To whom all correspondence should be addressed. zhuyanwu@ustc.edu.cn

[1] K. S. Novoselov, V. Fal, L. Colombo, P. Gellert, M. Schwab, and K. Kim, A roadmap for graphene, Nature (London) **490**, 192 (2012).
[2] Y. Chen, Y. Li, Y. Zhao, H. Zhou, and H. Zhu, Highly efficient hot electron harvesting from graphene before electron-hole thermalization, Sci. Adv. **5**, eaax9958 (2019).
[3] H. A. Hafez, S. Kovalev, J.-C. Deinert, Z. Mics, B. Green, N. Awari, M. Chen, S. Germanskiy, U. Lehnert, and J. Teichert, Extremely efficient terahertz high-harmonic generation in graphene by hot Dirac fermions, Nature (London) **561**, 507 (2018).
[4] M. Baudisch, A. Marini, J. D. Cox, T. Zhu, F. Silva, S. Teichmann, M. Massicotte, F. Koppens, L. S. Levitov, and F. J. G. de Abajo, Ultrafast nonlinear optical response of Dirac fermions in graphene, Nat. Commun. **9**, 1018 (2018).
[5] S. Tani, F. Blanchard, and K. Tanaka, Ultrafast Carrier Dynamics in Graphene under a High Electric Field, Phys. Rev. Lett. **109**, 166603 (2012).
[6] N. M. Gabor, J. C. Song, Q. Ma, N. L. Nair, T. Taychatanapat, K. Watanabe, T. Taniguchi, L. S. Levitov, and P. Jarillo-Herrero, Hot carrier–assisted intrinsic photoresponse in graphene, Science **334**, 648 (2011).
[7] J. M. Dawlaty, S. Shivaraman, M. Chandrashekhar, F. Rana, and M. G. Spencer, Measurement of ultrafast carrier dynamics in epitaxial graphene, Appl. Phys. Lett. **92**, 042116 (2008).
[8] M. Breusing, S. Kuehn, T. Winzer, E. Malić, F. Milde, N. Severin, J. Rabe, C. Ropers, A. Knorr, and T. Elsaesser, Ultrafast nonequilibrium carrier dynamics in a single graphene layer, Phys. Rev. B **83**, 153410 (2011).
[9] D. Brida, A. Tomadin, C. Manzoni, Y. J. Kim, A. Lombardo, S. Milana, R. R. Nair, K. S. Novoselov, A. C. Ferrari, and G. Cerullo, Ultrafast collinear scattering and carrier multiplication in graphene, Nat. Commun. **4**, 1987 (2013).
[10] K.-J. Tielrooij, J. Song, S. A. Jensen, A. Centeno, A. Pesquera, A. Z. Elorza, M. Bonn, L. Levitov, and F. Koppens, Photoexcitation cascade and multiple hot-carrier generation in graphene, Nat. Phys. **9**, 248 (2013).
[11] A. Betz, S. H. Jhang, E. Pallecchi, R. Ferreira, G. Fève, J.-M. Berroir, and B. Plaçais, Supercollision cooling in undoped graphene, Nat. Phys. **9**, 109 (2013).
[12] M. Mittendorff, T. Winzer, E. Malic, A. Knorr, C. Berger, W. A. de Heer, H. Schneider, M. Helm, and S. Winnerl, Anisotropy of excitation and relaxation of photogenerated charge carriers in graphene, Nano Lett. **14**, 1504 (2014).
[13] S. Ulstrup, J. C. Johannsen, F. Cilento, J. A. Miwa, A. Crepaldi, M. Zacchigna, C. Cacho, R. Chapman, E. Springate, and S. Mammadov, Ultrafast Dynamics of Massive Dirac Fermions in Bilayer Graphene, Phys. Rev. Lett. **112**, 257401 (2014).
[14] M. T. Mihnev, J. R. Tolsma, C. J. Divin, D. Sun, R. Asgari, M. Polini, C. Berger, W. A. De Heer, A. H. MacDonald, and T. B. Norris, Electronic cooling via interlayer Coulomb coupling in multilayer epitaxial graphene, Nat. Commun. **6**, 8105 (2015).
[15] H. Wang, J. H. Strait, P. A. George, S. Shivaraman, V. B. Shields, M. Chandrashekhar, J. Hwang, F. Rana, M. G. Spencer, and C. S. Ruiz-Vargas, Ultrafast relaxation dynamics of hot optical phonons in graphene, Appl. Phys. Lett. **96**, 081917 (2010).
[16] D. Sun, C. Divin, C. Berger, W. A. De Heer, P. N. First, and T. B. Norris, Spectroscopic Measurement of Interlayer Screening in Multilayer Epitaxial Graphene, Phys. Rev. Lett. **104**, 136802 (2010).
[17] D. Sun, Z.-K. Wu, C. Divin, X. Li, C. Berger, W. A. de Heer, P. N. First, and T. B. Norris, Ultrafast Relaxation of Excited Dirac Fermions in Epitaxial Graphene Using Optical Differential Transmission Spectroscopy, Phys. Rev. Lett. **101**, 157402 (2008).
[18] Z. Li, C. H. Lui, E. Cappelluti, L. Benfatto, K. F. Mak, G. L. Carr, J. Shan, and T. F. Heinz, Structure-Dependent Fano Resonances in the Infrared Spectra of Phonons in Few-Layer Graphene, Phys. Rev. Lett. **108**, 156801 (2012).
[19] W.-K. Tse and S. D. Sarma, Energy relaxation of hot Dirac fermions in graphene, Phys. Rev. B **79**, 235406 (2009).
[20] J. C. Song, M. Y. Reizer, and L. S. Levitov, Disorder-Assisted Electron-Phonon Scattering and Cooling Pathways in Graphene, Phys. Rev. Lett. **109**, 106602 (2012).

[21] D. Sun, Z. K. Wu, C. Divin, X. Li, C. Berger, W. A. d. Heer, P. N. First, and T. B. Norris, Ultrafast dynamics and interlayer thermal coupling of hot carriers in epitaxial graphene, Phys. Status Solidi C **6**, 470 (2009).
[22] Y. Zhang, T.-T. Tang, C. Girit, Z. Hao, M. C. Martin, A. Zettl, M. F. Crommie, Y. R. Shen, and F. Wang, Direct observation of a widely tunable bandgap in bilayer graphene, Nature (London) **459**, 820 (2009).
[23] Y. Cao, V. Fatemi, S. Fang, K. Watanabe, T. Taniguchi, E. Kaxiras, and P. Jarillo-Herrero, Unconventional superconductivity in magic-angle graphene superlattices, Nature (London) **556**, 43 (2018).
[24] Y. Cao, V. Fatemi, A. Demir, S. Fang, S. L. Tomarken, J. Y. Luo, J. D. Sanchez-Yamagishi, K. Watanabe, T. Taniguchi, and E. Kaxiras, Correlated insulator behaviour at half-filling in magic-angle graphene superlattices, Nature (London) **556**, 80 (2018).
[25] J. Gonzalez and T. Stauber, Kohn-Luttinger Superconductivity in Twisted Bilayer Graphene, Phys. Rev. Lett. **122**, 026801 (2019).
[26] X. Meng, T. Pandey, J. Jeong, S. Fu, J. Yang, K. Chen, A. Singh, F. He, X. Xu, and J. Zhou, Thermal Conductivity Enhancement in MoS_2 under Extreme Strain, Phys. Rev. Lett. **122**, 155901 (2019).
[27] F. Ke, Y. Chen, K. Yin, J. Yan, H. Zhang, Z. Liu, S. T. John, J. Wu, H.-k. Mao, and B. Chen, Large bandgap of pressurized trilayer graphene, Proc. Natl. Acad. Sci. U.S.A. **116**, 9186 (2019).
[28] See Supplemental Material at http://link.aps.org/supplemental/10.1103/PhysRevLett.126.027402 for the experimental and simulation methods and other supplementary figures.
[29] Z. Tao, J. Du, Z. Qi, K. Ni, S. Jiang, and Y. Zhu, Raman spectroscopy study of sp^2 to sp^3 transition in bilayer graphene under high pressures, Appl. Phys. Lett. **116**, 133101 (2020).
[30] J. M. Braun, H. Schneider, M. Helm, R. Mirek, L. A. Boatner, R. E. Marvel, R. F. Haglund, Jr., and A. Pashkin, Ultrafast response of photoexcited carriers in VO_2 at high-pressure, New J. Phys. **20**, 083003 (2018).
[31] A. Tomadin, D. Brida, G. Cerullo, A. C. Ferrari, and M. Polini, Nonequilibrium dynamics of photoexcited electrons in graphene: Collinear scattering, Auger processes, and the impact of screening, Phys. Rev. B **88**, 035430 (2013).
[32] H. Wang, C. Zhang, and F. Rana, Ultrafast dynamics of defect-assisted electron–hole recombination in monolayer MoS_2, Nano Lett. **15**, 339 (2015).
[33] Y. Wu, H. Chou, H. Ji, Q. Wu, S. Chen, W. Jiang, Y. Hao, J. Kang, Y. Ren, R. D. Piner, and R. S. Ruoff, Growth mechanism, and controlled synthesis of AB-stacked bilayer graphene on Cu-Ni alloy foils, ACS Nano **6**, 7731 (2012).
[34] J. Song, F.-Y. Kam, R.-Q. Png, W.-L. Seah, J.-M. Zhuo, G.-K. Lim, P. K. Ho, and L.-L. Chua, A general method for transferring graphene onto soft surfaces, Nat. Nanotechnol. **8**, 356 (2013).
[35] J. Hafner, Ab-initio simulations of materials using VASP: Density-functional theory and beyond, J. Comput. Chem., **29** 2044 (**2008**).
[36] P. E. Blöchl, Projector augmented-wave method, Phys. Rev. B **50**, 17953 (1994).
[37] S. Grimme, J. Antony, S. Ehrlich, and H. Krieg, A consistent and accurate ab initio parametrization of density functional dispersion correction (DFT-D) for the 94 elements H-Pu, J. Chem. Phys. **132**, 154104 (2010).
[38] S. Grimme, S. Ehrlich, and L. Goerigk, Effect of the damping function in dispersion corrected density functional theory, J. Comput. Chem. **32**, 1456 (2011).
[39] Q. Zheng, W. Chu, C. Zhao, L. Zhang, H. Guo, Y. Wang, X. Jiang, and J. Zhao, Ab initio nonadiabatic molecular dynamics investigations on the excited carriers in condensed matter systems, Wiley Interdiscip. Rev. **9**, e1411 (2019).
[40] J.-B. Wu, M.-L. Lin, X. Cong, H.-N. Liu, and P.-H. Tan, Raman spectroscopy of graphene-based materials and its applications in related devices, Chem. Soc. Rev. **47**, 1822 (2018).
[41] M. Hanfland, H. Beister, and K. Syassen, Graphite under pressure: Equation of state and first-order Raman modes, Phys. Rev. B **39**, 12598 (1989).
[42] R. Cuscó, J. Pellicer-Porres, J. H. Edgar, J. Li, A. Segura, and L. Artús, Pressure dependence of the interlayer and intralayer E_{2g} Raman-active modes of hexagonal BN up to the wurtzite phase transition, Phys. Rev. B **102**, 075206 (2020).
[43] G. Wang, Z. Dai, Y. Wang, P. Tan, L. Liu, Z. Xu, Y. Wei, R. Huang, and Z. Zhang, Measuring Interlayer Shear Stress in Bilayer Graphene, Phys. Rev. Lett. **119**, 036101 (2017).
[44] P. Tan, W. Han, W. Zhao, Z. Wu, K. Chang, H. Wang, Y. Wang, N. Bonini, N. Marzari, and N. Pugno, The shear mode of multilayer graphene, Nat. Mater. **11**, 294 (2012).
[45] R. Bistritzer and A. H. MacDonald, Electronic Cooling in Graphene, Phys. Rev. Lett. **102**, 206410 (2009).
[46] Q. Zheng, Y. Xie, Z. Lan, O. V. Prezhdo, W. A. Saidi, and J. Zhao, Phonon-coupled ultrafast interlayer charge oscillation at van der Waals heterostructure interfaces, Phys. Rev. B **97**, 205417 (2018).
[47] Y. Wang, Y. Shi, C. Zhao, Q. Zheng, and J. Zhao, Photogenerated carrier dynamics at the anatase/rutile TiO_2 interface, Phys. Rev. B **99**, 165309 (2019).
[48] X. Niu, Y. Li, Y. Zhang, Q. Li, Q. Zhou, J. Zhao, and J. Wang, Photo-oxidative degradation and protection mechanism of black phosphorus: Insights from ultrafast dynamics, J. Phys. Chem. Lett. **9**, 5034 (2018).